■文　献

1) Committee of Brain Tumor Registry of Japan: Report of Brain Tumor Registry of Japan (1969–1996). Neurol Med Chir (Tokyo) **43** (Suppl i–vii): 1–111, 2003.
2) 川　茂幸：XI. 腫瘍マーカーの検査．臨床検査法提要，第6章　臨床化学検査（金井　泉原著），p668–682，金原出版，1998.
3) Patchell RA, et al: A randomized trial of surgery in the treatment of single metastases to the brain. N Engl J Med **322**: 494–500, 1990.
4) Noordijk EM, et al: The choice of treatment of single brain metastasis should be based on extracranial tumor activity and age. Int J Radiat Oncol Biol Phys **29**: 711–717, 1994.
5) Zimm S, et al: Intracerebral metastases in solid-tumor patients: natural history and results of treatment. Cancer **48**: 384–394, 1981.
6) Lagerwaard FJ, et al: Identification of prognostic factors in patients with brain metastases: a review of 1292 patients. Int J Radiat Oncol Biol Phys **43**: 795–803, 1999.
7) DeAngelis LM, et al: Radiation-induced dementia in patients cured of brain metastases. Neurology **39**: 789–796, 1989.
8) Johnson BE, et al: Neurologic, neuropsychologic, and computed cranial tomography scan abnormalities in 2- to 10-year survivors of small-cell lung cancer. J Clin Oncol **3**: 1659–1667, 1985.
9) Sheehan JP, et al: Radiosurgery for non-small cell lung carcinoma metastatic to the brain: long-term outcomes and prognostic factors influencing patient survival time and local tumor control. J Neurosurg **97**: 1276–1281, 2002.
10) Andrews DW, et al: Whole brain radiation therapy with or without stereotactic radiosurgery boost for patients with one to three brain metastases: phase III results of the RTOG 9508 randomised trial. Lancet **363**: 1665–1672, 2004.
11) Kondziolka D, et al: Stereotactic radiosurgery plus whole brain radiotherapy versus radiotherapy alone for patients with multiple brain metastases. Int J Radiat Oncol Biol Phys **45**: 427–434, 1999.
12) Li B, et al: Comparison of three treatment options for single brain metastasis from lung cancer. Int J Cancer **90**: 37–45, 2000.
13) Aoyama H, et al: Interim report of the JROSG99-1 multi-institutional randomized trial, comparing radiosurgery alone vs. radiosurgery plus whole brain irradiation for 1–4 brain metastases. Proceedings of 40th annual meeting of American society of clinical oncology. J Clin Oncol **22**: 108, 2004.
14) 嘉山孝正：転移性脳腫瘍に対する標準的治療法確立に関する研究．平成15年度厚生労働科学研究がん分野研究成果発表会（研究者向け）報告書，p13–15，2004.

Available online at www.sciencedirect.com

SCIENCE DIRECT

Surgical Neurology 63 (2005) 56–61

SURGICAL NEUROLOGY

www.surgicalneurology-online.com

Imaging

Fractional anisotropy value by diffusion tensor magnetic resonance imaging as a predictor of cell density and proliferation activity of glioblastomas

Takaaki Beppu, MD[a,*], Takashi Inoue, MD[a], Yuji Shibata, PhD[b], Noriyuki Yamada, PhD[c], Akira Kurose, MD[b], Kuniaki Ogasawara, MD[a], Akira Ogawa, MD[a], Hiroyuki Kabasawa, DEng[d]

Departments of [a]Neurosurgery, [b]First Department of Pathology, and [c]Clinical Pathology, Iwate Medical University, Morioka 020-8505, Japan

[d]GE Yokogawa Medical Systems, Tokyo, Japan

Received 4 March 2003; accepted 12 February 2004

Abstract

Background: In vivo, water diffusion displays directionality due to presence of complex microstructural barriers in tissue. The extent of directionality of water diffusion can be expressed as a fractional anisotropy (FA) value using diffusion tensor magnetic resonance imaging (DTI). The FA value has been suggested as an indicator of the cell density of astrocytic tumors. The aim of the present study was to confirm beyond doubt that FA values indicate cell density even when limited in glioblastomas and to determine whether the FA value of a given patient predicts proliferation activity in the individual glioblastoma.

Methods: We performed DTI in 19 patients with glioblastoma and measured the FA values of tumor and normal brain regions prior to computed tomography–guided stereotactic biopsy. Differences in mean FA value between normal brain regions and glioblastoma lesion were compared. Cell density and MIB-1 indices were examined using tumor specimens obtained from biopsies. Correlation among FA values, cell density, and MIB-1 indices was also evaluated.

Results: The mean FA value significantly differed between normal brain regions and glioblastoma lesions. Positive correlation was observed between FA value and cell density ($r = 0.73$, $P < 0.05$) and between FA value and MIB-1 index ($r = 0.80$, $P < 0.05$).

Conclusions: Our results suggest that the FA value of glioblastoma as determined by DTI prior to surgery is a good predictor of cell density and, consequently, proliferation activity.

Keywords: Cell density; Diffusion tensor magnetic resonance imaging; Fractional anisotropy; Glioblastoma; Proliferation

1. Introduction

Essentially, the diffusion of water molecules displays microscopic random (Brownian) translational motion, and under these conditions, the molecular mobility of water is the same in all directions. In vivo, water diffusion takes on an abnormal motion due to hindrance by the presence of complex microstructural barriers in tissue, such as white matter tracts, cell membranes, and/or capillary vessels, and consequently the change in magnitude and directionality of water diffusion arises in a 3-dimensional space [2]. This directional variation is termed diffusion anisotropy. Diffusion tensor magnetic resonance imaging (DTI) provides quantitative information about the magnitude and directionality of water diffusion along a vector in a 3-dimensional space [4,6,17,26]. Evaluation of directionality of water diffusion using DTI has recently become available for visualization of cerebral fiber tracts [26] and demonstration of substantial differences among the various lesions of multiple sclerosis [1,7,8,24]. In DTI, a set of orthogonal vectors known as eigenvectors, which define the orientation of the principal axes of a diffusion ellipsoid in space, are

* Corresponding author. Tel.: +81 196 51 5111x6603; fax: +81 196 25 8799.

E-mail address: tbeppu@iwate-med.ac.jp (T. Beppu).

0090-3019/$ – see front matter © 2005 Elsevier Inc. All rights reserved.
doi:10.1016/j.surneu.2004.02.034

calculated from the diffusion tensor. The length of each vector is represented by corresponding eigenvalues. The fractional anisotropy (FA) is derived from eigenvectors for quantification of anisotropy. A FA value is calculated using the following formula based on eigenvalues in the diffusion tensor [2,18]:

$$FA = \sqrt{\frac{3}{2}} \frac{\sqrt{(\lambda_1 - \langle D \rangle)^2 + (\lambda_2 - \langle D \rangle)^2 + (\lambda_3 - \langle D \rangle)^2}}{\sqrt{\lambda_1^2 + \lambda_2^2 + \lambda_3^2}} \cdots \quad (1)$$

$$\langle D \rangle = \frac{1}{3}(\lambda_1 + \lambda_2 + \lambda_3) \cdots \quad (2)$$

where λ_1, λ_2, and λ_3 are the largest, intermediate, and smallest eigenvalues, respectively, of the diffusion tensor. The FA is expressed as a numerical value between 0 and 1 without a unit. A higher FA value implies a greater degree of anisotropic motion of water molecules.

Presurgical knowledge of the cell density and proliferation potential of the tumor tissue would have prognostic significance and help to elucidate the histologic characteristics in individual patients with astrocytic tumors. Water diffusion has been suggested to be affected by tumor cellularity in gliomas [22]. Our preliminary study suggested a correlation between the FA value and the tumor cell density or malignancy grades in astrocytic tumors [3], which led to the presumption that FA values also correlate with the cell proliferation activity of astrocytic tumors. To date, whether FA can act as an indicator of cell proliferation in astrocytic tumors is unknown. The quantitative estimation of cell density or proliferation is largely complicated by widely distributed values of differently graded astrocytic tumors when a study involves a group of mixed, differently graded tumors. To confirm whether FA values indicate cell density and proliferation activity of an astrocytic tumor group limited to 1 type, we examined the relationship among FA value, tumor cell density, and MIB-1 index, which is widely used as a quantitative information of cell proliferation [10,12,19,25] in glioblastomas alone.

2. Materials and methods

2.1. Patient population

The study protocol was approved by the Ethics Committee of Iwate Medical University (Morioka, Japan). The patients recruited to this study were admitted to the Department of Neurosurgery, Iwate Medical University, between September 2000 and December 2002. Entry criteria for this study were as follows: (A) adult patients who were diagnosed with supratentorial glioblastoma; (B) patients whose tumor was primarily in the cerebral white matter, except for the basal ganglia, corpus callosum, ventricle, and brain stem; (C) patients who received routine magnetic resonance imaging (MRI) and DTI within the 2 weeks prior to computed tomography–guided stereotactic biopsy; and (D) informed written consent to participate. Diagnosis was based on the histologic features of specimens obtained from a stereotactic biopsy according to the World Health Organization classification [13]. A total of 19 patients (11 males and 8 females; mean age, 58.9 years; age range, 28-77 years) participated. The main tumor sites were the frontal lobe in 6 patients, parietal lobe in 7, temporal lobe in 5, and occipital lobe in 1.

2.2. Measurement of FA value

All routine MRI and DTI scans were performed using a 3.0 T MRI system (Signa VH/I, GE Medical Systems, Milwaukee, WI) with a standard head coil. A spin echo–type echo planar imaging sequence with diffusion gradients applied in 6 directions was used for the diffusion tensor imaging: repetition time 10,000 ms, echo time 84 ms, matrix 256 × 260, field of view 240 mm^2, 6 mm thickness, 2 mm gap, b factors 800 s/mm^2. All patients also underwent conventional spin echo T1- and T2-weighted imaging prior to DTI and T1-weighted imaging with contrast medium after DTI. All image analysis after processing was performed on a scanner console using a subprogram of the Functool image analysis software (GE Medical Systems, Buc, France) modified by one of the investigators (HK).

The region of interest (ROI) was determined on a slice showing maximal tumor size in T1-weighted imaging with contrast medium, because the tumors of all patients were detected as enhancing lesions. Where possible, the ROI was placed at the enhancing central region of the tumor. If central necrosis was evident, the ROI was placed on a ring-enhancing region of the tumor containing more metabolically active sites than the central region (Fig. 1A). The ROI was also placed in subcortical normal white matter (NWM) where no abnormalities on T2-weighted MRI were detected. When the tumor was sited in the frontal lobe or anterior half of the temporal lobe, the ROI was placed in subcortical white matter of the contralateral occipital lobe. On the other hand, the ROI was placed in subcortical white matter of the contralateral frontal lobe when the tumor was situated in the parietal lobe, the occipital lobe, or the posterior half of the temporal lobe. If the tumor was not in or had not infiltrated into the corpus callosum on T2-weighted MRI, the ROI was placed at the genu or splenium of the corpus callosum. When the tumor was sited in the frontal lobe or anterior half of the temporal lobe, the ROI was placed in the splenium, whereas the ROI was placed in the genu when the tumor was situated in the parietal lobe, the occipital lobe, or the posterior half of the temporal lobe. ROIs were automatically transferred onto the coregistered FA maps constructed from DTI (Fig. 1B, C). The FA values were then calculated for each patient using the modified Functool image analysis software. The FA value was identified as a mean of values derived for every pixel in a

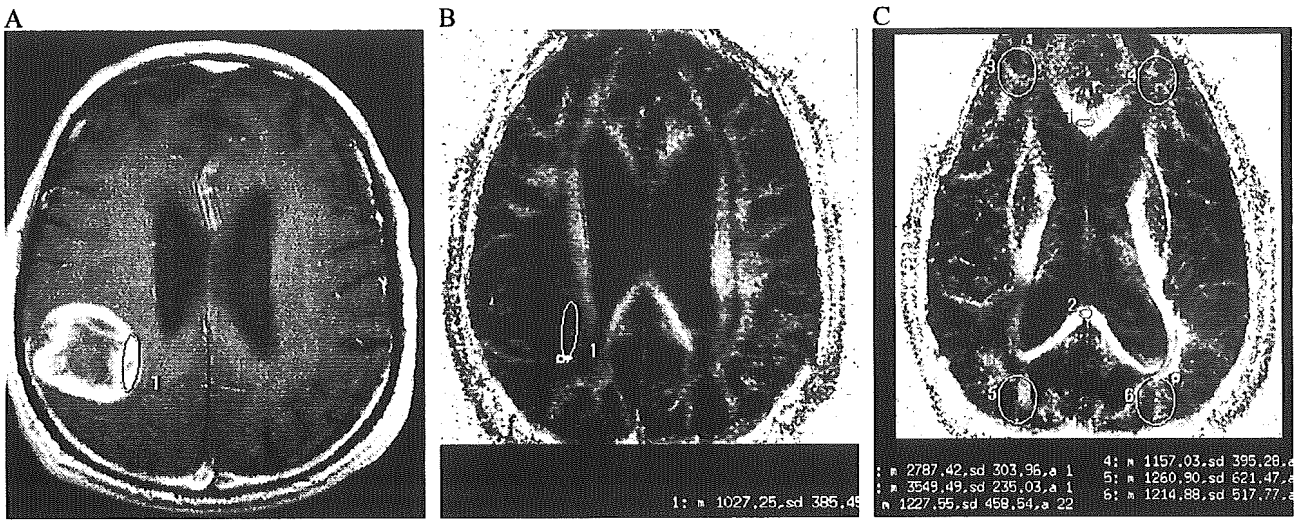

Fig. 1. Locations of ROI in a patient with glioblastoma of the right parietal lobe. A, Gadolinium-enhanced T1-weighted MR image. Circle, ROI within a ring-enhancing lesion of the tumor. B, The coregistered FA maps from DTI. The ROI that was determined from the gadolinium-enhanced T1-weighted MR image was transferred onto a FA map. C, FA map for NWM. Because the tumor was situated in the parietal lobe, only FA values in ROIs of the contralateral frontal lobe (No 4) and the genu (No 1) were accepted.

given ROI. All MRI and DTI procedures were performed by 1 investigator (TI).

2.3. Tumor tissue specimens

In all patients, the tumor tissue specimens were obtained by computed tomography–guided stereotactic biopsy targeted to the intratumoral area corresponding exactly to the ROI within which the FA value was measured. For patients who underwent tumor resection with a large craniotomy, stereotactic biopsy was performed prior to tumor resection. In these patients, a silicon tube was left in the intracerebral trajectory made by the biopsy and was then used as a guide for tumor localization during tumor resection.

After biopsy, specimens were immediately fixed in 30% formalin for 24 hours at room temperature and then embedded in paraffin. Each paraffin block was cut into 6-μm-thick serial sections that were used for hematoxylin and eosin staining and Ki-67 immunohistochemical staining. Cell density was identified as the mean of tumor cell numbers in hematoxylin and eosin–stained preparations in 10 fields of a square 25 μm per side under 200 × magnification. Ki-67 was immunohistochemically detected using anti-Ki-67 monoclonal antibody (MIB-1, DAKO, Copenhagen, Denmark) diluted 1:50 and was stained by the modified avidin-biotin-peroxidase complex method [11]. Prior to Ki-67 immunohistochemical staining, sections were treated in an autoclave at 121°C for 15 minutes. The percentage of stained positive cells in approximately 1000 cells, except for inflammatory cells and vascular cells, under a light microscope (200 ×) was defined as the MIB-1 index for that patient. All histologic analyses were performed by 3 investigators (YS, NY, and AK) with no prior knowledge of the patient data.

2.4. Statistical analysis

Mean FA values of subcortical NWM, normal corpus callosum, and glioblastoma tissue were calculated and then compared statistically using 1-factor ANOVA. Correlation among FA values, cell density, and MIB-1 indices of glioblastoma tissues was analyzed statistically using Pearson's correlation coefficient. Statistical significance was established at the $P < 0.05$ level.

3. Results

The mean FA values of the corpus callosum (the genu in 9 patients and the splenium in 10 patients), subcortical white

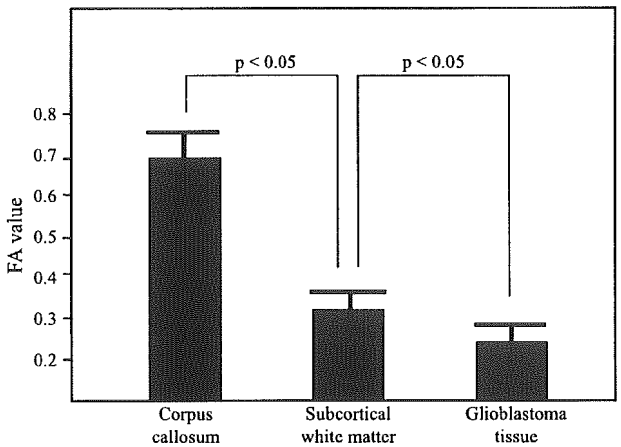

Fig. 2. Mean FA values of regions in NWM and glioblastoma. Significant differences in mean FA values were observed between the corpus callosum, subcortical white matter and glioblastoma lesion.

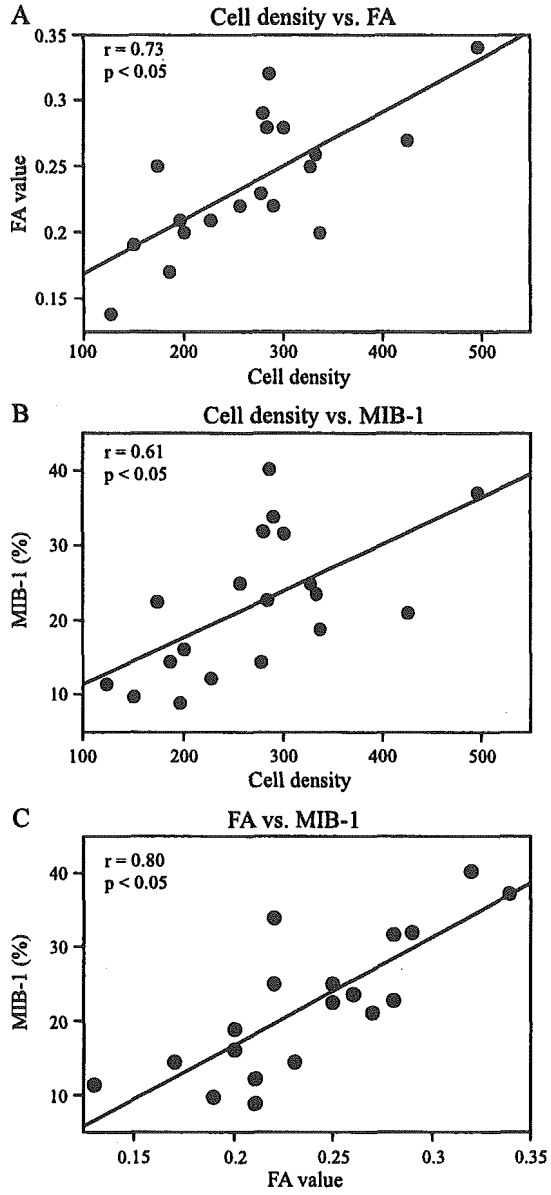

Fig. 3. Correlation between FA value and cell density (A), between cell density and MIB-1 index (B), and between FA value and MIB-1 index (C) in all patients. Strong correlation was observed between FA value and cell density (A) and between FA value and MIB-1 index (C), whereas correlation between cell density and MIB-1 index was moderate (B).

matter (the frontal lobe in 9 patients and the occipital lobe in 10 patients), and glioblastoma lesion were 0.70 ± 0.05, 0.32 ± 0.04, and 0.24 ± 0.05, respectively. The mean FA values were significant different among the corpus callosum, subcortical white matter, and glioblastoma tissue ($P < 0.05$; Fig. 2).

In glioblastoma lesions, the mean values of cell density and MIB-1 index were 270 ± 93% and 21.6 ± 10.0%, respectively. Strong correlation was observed between FA value and cell density ($r = 0.73$, $P < 0.05$) and between FA value and MIB-1 index ($r = 0.80$, $P < 0.05$; Fig. 3A, C), whereas there was moderate correlation between cell density and MIB-1 index ($r = 0.61$, $P < 0.05$; Fig. 3B).

4. Discussion

Normal white matter shows strong directionality of water diffusion and, consequently, a high FA value, because the water diffusion parallel to the white matter tracts is less restricted than the water diffusion perpendicular to them [26]. Although limited information is available for the subcortical NWM and corpus callosum, FA values are 0.2 to 0.6 in the frontal lobe [7,8,21,24,28] and 0.6 to 0.8 in the corpus callosum [1,7,8,16,21]. The FA values in the present study for the subcortical NWM and corpus callosum were similar to those reports (Fig. 2), confirming the reliability of the FA values obtained here. On the other hand, the FA values of glioblastoma tissue have been reported to be lower than those of NWM [20], which is consistent with our result. When astrocytic tumors grow in white matter, almost all normal fiber and cell structures are destroyed by the tumor nidus or displaced and separated to surround the tumor nidus [27]. One possible explanation for the lower mean FA values of the tumor core than NWM is that destruction or displacement of normal fibers induces a decrease in the directionality of water diffusion and a relative decrease in FA value [3,20].

FA value is thought to be largely affected by tumor cell density in glioma tissue [20]. Our preliminary study reported that higher anaplastic grade and higher cell density increased the FA value of differently graded gliomas [3]. The present study indicated that FA values strongly correlated with cell density even when the analysis was limited to glioblastomas alone (Fig. 3A). We hypothesized that the FA value of astrocytic tumor tissue is determined by a balance between factors decreasing the degree of the directionality of water diffusion, such as fiber destruction or displacement, and factors increasing it, such as high cell density and/or vascularity [3]. Even in a study group limited to glioblastomas, cell density rather than normal fiber tracts would predominantly affect FA value, as normal fibers are completely destroyed or displaced to around the tumor core. In the present study, FA value strongly correlated with MIB-1 index (Fig. 3C). This finding could be arrived by syllogism (ie, correlation between FA value and cell density and between cell density and MIB-1 index) and allows the assumption of correlation between FA value and MIB-1 index. The correlation between FA value and MIB-1 index suggests that the FA value predicts not only cell density but also proliferation activity in glioblastomas. Although there is general consensus that MIB-1 index does not allow a prognosis in individual patients with glioblastoma [13], we believe that prediction of proliferation activity prior to surgery would be helpful for the diagnosis and characterization of glioblastomas.

Why FA value, which is an indicator of directionality of water diffusion, correlates strongly with cell density in glioblastoma tissue is unclear. Using diffusion-weighted MRI, evaluations of water diffusion in gliomas or the other

brain tumors have been documented previously [4,5,9,14, 15,22,23]. All authors reported that the value of the apparent diffusion coefficient, which is an indicator of the magnitude of water diffusion, decreased with tumor cell density. The apparent diffusion coefficient values negatively correlated to the cell density in both glioblastomas and diffuse astrocytomas [14]. Furthermore, low apparent diffusion coefficient value in gliomas reflects a decreased volume of extracellular space, which accelerates water diffusion due to encroachment by tumor cells, and/or an increased intracellular viscosity [5,22]. Similarly, we speculate that 1 possible reason for the correlation between FA value and cell density is that an increased amount of cellular membranes and intracellular viscosity, as well as relatively decreased extracellular space in glioblastoma tissue, also induces an increase in the extent of directionality of water diffusion within each pixel of DTI, resulting in a relative increase in FA value.

The present study possesses some limitations regarding interpretation of the FA values. First, how structural factors other than cell density (eg, vascularity, edema, microcysts, tumor cell size, bipolar processes of neoplastic cells, and velocity of flowing blood in capillaries) affect the directionality of water diffusion and alter FA values was not explored. Although the present results suggest that primarily cell density affects FA value, these other factors may also affect it to some small extent. This issue is a matter for future analysis. Second, the present results do not apply to the invading lesion around a tumor nidus. Within such lesions, tumor cells infiltrate along myelinated fibers and disrupt normal cell structure [13]. It is not clear how the directionality of water diffusion and FA are affected by preserved fiber tracts, normal cell structure, and vigorous edema in peritumoral regions. Third, the present results do not apply to brain tumors other than glioblastoma, because the histologic structures of the other tumors differ from those of glioblastoma. For example, the FA value of gliomatosis cerebri with moderate cell density is equivalent to that of glioblastoma, because preservation of normal axons increases the extent of directionality of water diffusion [3]. Correlation of FA value with cell density and proliferation activity is required for each tumor using a study group limited to 1 type.

In conclusion, our findings suggested that the FA value of glioblastoma is determined at the very least by cell density and, consequently, correlates with proliferation activity, although the sample size of the present study was small. Measurement of FA value using DTI will most likely become an option for auxiliary examinations prior to surgery for glioblastoma.

Acknowledgments

This study was supported in part by a grant-in-aid for Advanced Medical Science Research from the Ministry of Science, Education, Sports and Culture, Japan.

References

[1] Bammer R, Augustin M, Strasser-Fuchs S, Seifert T, Kapeller P, Stollberger R, Ebner F, Hartung HP, Fazekas F. Magnetic resonance diffusion tensor imaging for characterizing diffuse and focal white matter abnormalities in multiple sclerosis. Magn Reson Med 2000; 44:583-91.

[2] Basser PJ, Pierpaoli C. Microstructural and physiological features of tissues elucidated by quantitative-diffusion-tensor MRI. J Magn Reson B 1996;111(3):209-19.

[3] Beppu T, Inoue T, Shibata Y, Kurose A, Arai H, Ogasawara K, Ogawa A, Nakamura S, Kabasawa H. Measurement of fractional anisotropy using diffusion tensor MRI in supratentorial astrocytic tumors. J Neurooncol 2003;63:109-16.

[4] Brunberg JA, Chenevert TL, McKeever PE, Ross DA, Junck LR, Muraszko KM, Dauser R, Pipe JG, Betley AT. In vivo MR determination of water diffusion coefficients and diffusion anisotropy: correlation with structural alteration in gliomas of the cerebral hemispheres. AJNR Am J Neuroradiol 1995;16:361-71.

[5] Castillo M, Smith JK, Kwock L, Wilber K. Apparent diffusion coefficients in the evaluation of high-grade cerebral gliomas. AJNR Am J Neuroradiol 2001;22(1):60-4.

[6] Chien D, Kwong KK, Gress DR, Buonanno FS, Buxton RB, Rosen BR. MR diffusion imaging of cerebral infarction in humans. AJNR Am J Neuroradiol 1992;13:1097-105.

[7] Ciccarelli O, Werring DJ, Wheeler-Kingshott CAM, Barker GJ, Parker GJM, Thompson AJ, Miller DH. Investigation of MS normal-appearing brain using diffusion tensor MRI with clinical correlations. Neurology 2001;56:926-33.

[8] Filippi M, Cercignani M, Inglese M, Horsfield MA, Comi G. Diffusion tensor magnetic resonance imaging in multiple sclerosis. Neurology 2001;56:304-11.

[9] Filippi CG, Edgar MA, Ulug AM, Prowda JC, Heier LA, Zimmerman RD. Appearance of meningiomas on diffusion-weighted images: correlating diffusion constants with histopathologic findings. AJNR Am J Neuroradiol 2001;22(1):65-72.

[10] Heesters MA, Koudstaal J, Go KG, Molenaar WM. Proliferation and apoptosis in long-term surviving low grade gliomas in relation to radiotherapy. J Neurooncol 2002;58:157-65.

[11] Hsu SM, Raine L, Fanger H. Use of avidin-biotin-peroxidase complex (ABC) in immunoperoxidase techniques: a comparison between ABC and unlabeled antibody (PAP) procedures. J Histochem Cytochem 1981;29:577-80.

[12] Karamitopoulou E, Perentes E, Diamantis I, Maraziotis T. Ki-67 immunoreactivity in human central nervous system tumors: a study with MIB 1 monoclonal antibody on archival material. Acta Neuropathol (Berl) 1994;87(1):47-54.

[13] Kleihues P, Cavenee WK. World Health Organization classification of tumours: pathology and genetics, tumours of the nervous system. Lyon: International Agency for Research on Cancer (IARC); 2000. p. 6-92.

[14] Kono K, Inoue Y, Nakayama K, Shakudo M, Morino M, Ohata K, Wakasa K, Yamada R. The role of diffusion-weighted imaging in patients with brain tumors. AJNR Am J Neuroradiol 2001;22(6): 1081-8.

[15] Krabbe K, Gideon P, Wagn P, Hansen U, Thomsen C, Madsen F. MR diffusion imaging of human intracranial tumours. Neuroradiology 1997;39(7):483-9.

[16] Melhem ER, Itoh R, Jones L, Barker PB. Diffusion tensor MR imaging of the brain: effect of diffusion weighting on trace and anisotropy measurements. AJNR Am J Neuroradiol 2000;21:1813-20.

[17] Pierpaoli C, Jezzard P, Basser PJ, Barnett A, Di Chiro G. Diffusion tensor MR imaging of the human brain. Radiology 1996;201:637-48.

[18] Pierpaoli C, Basser PJ. Toward a quantitative assessment of diffusion anisotropy. Magn Reson Med 1996;36(6):893-906.

[19] Schroder R, Feisel KD, Ernestus RI. Ki-67 labeling is correlated with the time to recurrence in primary glioblastomas. J Neurooncol 2002; 56:127-32.

[20] Sinha S, Bastin ME, Whittle IR, Wardlaw JM. Diffusion tensor MR imaging of high-grade cerebral gliomas. AJNR Am J Neuroradiol 2002;23(4):520-7.
[21] Sorensen AG, Buonanno FS, Gonzalez RG, Schwamm LH, Lev MH, Huang-Hellinger FR, Reese TG, Weisskoff RM, Davis TL, Suwanwela N, Can U, Moreira JA, Copen WA, Look RB, Finklestein SP, Rosen BR, Koroshetz WJ. Hyperacute stroke: evaluation with combined multisection diffusion-weighted and hemodynamically weighted echo-planar MR imaging. Radiology 1996;199(2):391-401.
[22] Sugahara T, Korogi Y, Kochi M, Ikushima I, Shigematu Y, Hirai T, Okuda T, Liang L, Ge Y, Komohara Y, Ushio Y, Takahashi M. Usefulness of diffusion-weighted MRI with echo-planar technique in the evaluation of cellularity in gliomas. J Magn Reson Imaging 1999;9:53-60.
[23] Tien RD, Felsberg GJ, Friedman H, Brown M, MacFall J. MR imaging of high-grade cerebral gliomas: value of diffusion-weighted echoplanar pulse sequences. AJR Am J Roentgenol 1994;162(3):671-7.
[24] Tievsky AL, Ptak T, Farkas J. Investigation of apparent diffusion coefficient and diffusion tensor anisotropy in acute and chronic multiple sclerosis lesions. AJNR Am J Neuroradiol 1999;20:1491-9.
[25] Wakimoto H, Aoyagi M, Nakayama T, Nagashima G, Yamamoto S, Tamaki M, Hirakawa K. Prognostic significance of Ki-67 labeling indices obtained using MIB-1 monoclonal antibody in patients with supratentorial astrocytomas. Cancer 1996;77(2):373-80.
[26] Witwer BP, Moftakhar R, Hasan KM, Deshmukh P, Haughton V, Field A, Arfanakis K, Noyes J, Moritz CH, Meyerand ME, Rowley HA, Alexander AL, Badie B. Diffusion-tensor imaging of white matter tracts in patients with cerebral neoplasm. J Neurosurg 2002;97:568-75.
[27] Yasargil MG. Microneurosurgery IV A [in 4 volumes]. Stuttgart/New York Verlag: Georg Thieme; 1993. p. 127 [for distribution in Japan: Nankodo Company Ltd Tokyo].
[28] Yoshiura T, Wu O, Zeheer A, Reese TG, Sorensen G. Highly diffusion-sensitized MRI of brain: dissociation of gray and white matter. Magn Reson Med 2001;45:734-40.

Commentary

In this interesting article, Beppu et al suggest that diffusion tensor imaging can be used to look at the disruption of fibers by an invasive tumor. This is a potentially important application of this novel technique to the analysis of brain tumors. At the Brigham and Women's Hospital, we have developed this technology primarily to assess to what degree low-grade tumors infiltrate rather than disrupt fibers. It has been an important tool for assessing the likelihood that surgery will cause new deficits in patients with these tumors.

The findings of Beppu et al are what we all might well believe—that glioblastomas are invasive tumors that significantly disrupt normal fiber tracts. Although the study has relatively few patients, the techniques are quite demanding and therefore worthwhile reading. This is a valuable addition to the literature of neurosurgical oncology to decide whether surgery should be done.

Peter M. Black, MD, PhD
Department of Neurosurgery
Children's Hospital
Boston, MA 02115, USA

Journal of Neuro-Oncology (2005) 73: 137–144
DOI 10.1007/s11060-004-3340-4

Clinical Study

Utility of three-dimensional anisotropy contrast magnetic resonance axonography for determining condition of the pyramidal tract in glioblastoma patients with hemiparesis

Takaaki Beppu[1], Takashi Inoue[1], Yasutaka Kuzu[1], Kuniaki Ogasawara[1], Akira Ogawa[1] and Makoto Sasaki[2]
[1]*Department of Neurosurgery;* [2]*Department of Radiology, Iwate Medical University, Morioka, Japan*

Key words: glioblastoma, pyramidal, tract, axonography,diffusion MRI

Summary

Background and purpose: Three-dimensional anisotropy contrast magnetic resonance axonography (3DAC) is a technique for diffusion weighted magnetic resonance imaging (DWI) that offers reliable visualization of the pyramidal tracts. This study evaluated condition of the pyramidal tract using 3DAC in glioblastoma patients with hemiparesis. *Methods:* In 18 glioblastoma patients before surgery, 3DAC findings of the pyramidal tract responsible for hemiparesis were compared with finding from proton density-weighted imaging (PDWI). To estimate extent of pyramidal tract destruction, fractional anisotropy (FA) values using diffusion tensor magnetic resonance imaging were examined for both the responsible and non-pathological pyramidal tracts. *Results*: In all five patients for whom PDWI indicated no hyperintense foci in the responsible pyramidal tract, 3DAC demonstrated no change in color. When PDWI revealed hyperintense foci, 3DAC showed two types of findings: no color change (five patients); or obscured dark area (six patients). When 3DAC showed a dark area, mean FA value in the responsible tract was significantly lower than that for the non-pathological tract. *Conclusion:* When PDWI indicates hyperintense foci on the pyramidal tract, 3DAC allows prediction of pyramidal tract condition, such as large tumor invasion.

Introduction

Developments in neuroimaging technology have enabled accurate preoperative evaluation of cerebral cortical function and integrity [1–5]. Evaluation of subcortical integrity is also necessary prior to surgery, as functional recovery after surgery may be limited by previous subcortical injury [6,7]. For example, decisions regarding surgical approach and predictions of individual performance status after surgery vary according to the cause of subcortical functional disorder, such as compression, invasion, or disruption of the subcortical tracts by glioma.

Diffusion-weighted imaging (DWI) and diffusion tensor imaging (DTI) are magnetic resonance imaging (MRI) techniques that provide quantitative information about the magnitude and direction of water diffusion, respectively, in a three-dimensional space. These techniques offer some advantages for evaluating subcortical structures comprising white matter tracts, since diffusion of water parallel to nerve fibers is less restricted than water diffusion perpendicular to the fibers [8–10]. Using DWI and DTI, the corticospinal tracts can be visualized as 'tractography' [11–16]. Three-dimensional anisotropy contrast magnetic resonance axonography (3DAC) using DWI is one method of tractography, and represents a reliable technique for visualizing anisotropic diffusion through nerve fibers [17,18]. Of the cerebral white matter nerve fiber tracts, the pyramidal tract is particularly suitable for 3DAC [18]. Currently, 3DAC allows clinical estimation of pyramidal tract status in patients with cerebral infarction or brain tumor [14,15,19,20]. In patients with glioma, tractography provides information on the localization of tumor bulk relative to the pyramidal tract. This useful information has been utilized in the field of brain tumor surgery [21–24]. When a tumor attaches to the pyramidal tract in a patient with hemiparesis, information on condition of the pyramidal tract adjacent to the tumor, such as compression, invasion or disruption by the tumor, is often desired for glioma resection. If 3DAC could provide not only information on localization of tumor bulk and the pyramidal tract, but also condition of the pyramidal tract, 3DAC would become even more useful for neuro-oncologists.

Proton density-weighted imaging (PDWI) on conventional MRI can obtain a high contrast between gray and white matter, and is used for visualization of the corticospinal tracts [25]. We compared PDWI findings in the pyramidal tract responsible for hemiparesis with findings from 3DAC. Furthermore, fractional anisotropy (FA) value was measured to estimate extent of the pyramidal tract destruction. FA value from DTI provides the best quantitative information regarding degree of directionality of water diffusion, and can thus indicate degree of nerve fiber destruction [16,26,27]. The present study aimed to determine the utility of 3DAC for estimating condition of the pyramidal tracts in patients with hemiparesis due to glioblastoma, and to define patient subgroups that would benefit from 3DAC.

Methods

Patients and clinical course

The study protocol was approved by the Ethics Committee of Iwate Medical University, Morioka, Japan. Patients recruited to this study were admitted to the Department of Neurosurgery at Iwate Medical University between September 2000 and March 2004. Entry criteria for this study were: adult (20 years old) patients who had been diagnosed with supratentorial glioblastoma mainly sited in the cerebral white matter excluding the primary motor cortex and brain stem; patients who presented with hemiparesis due to motor-related disorder of the pyramidal tract; and provision of written informed consent to participate. Diagnosis of glioblastoma was based on histological features of surgical specimens obtained after processing all image analyses. Patient data are summarized in Table 1. Subjects comprised 18 patients (six males, 12 females) with a mean age of 58.5 years (range, 31–77 years). Twelve patients were treated using either total or subtotal tumor removal, and six patients underwent only biopsy. Extent of hemiparesis before and after surgery was evaluated for the arm, finger and foot of each patient using Bruunstrom's grading system [28]. This system utilizes six stages, with stage 1 equal to severe hemiplegia and stage 6 representing basically normal strength. The lowest stage from the arm, finger or foot was used to define degree of hemiparesis for each patient. All patients underwent radiochemotherapy starting from 2 weeks after surgery. Postoperative hemiparesis was evaluated immediately before starting radiochemotherapy. Hemipareses before and after surgery were compared statistically. Values of $P < 0.05$ were considered statistically significant.

Conventional MRI

Conventional MRI was performed within 7 days before surgery. All patients underwent fast spin-echo PDWI and T2-weighted imaging (WI), and conventional spin-echo non-enhanced and gadolinium-enhanced T1-WI (Gd-T1WI) prior to DWI. Conventional MRI was performed using a 1.5-T whole body scanner (GE Yokogawa Medical Systems, Tokyo, Japan) and standard head coil. The pyramidal tract nearest the tumor on PDWI was defined as the tract responsible for hemiparesis. Estimations of the responsible tract using conventional MRI were performed using the criteria outlined below. Responsible tracts were classified into three groups according to PDWI: (1) 'clear' group in which tracts were clearly visualized without hyperintense foci; (2) 'hyperintense' group in which tracts displayed hyperintense foci; and (3) 'absent' group in which tracts could not be observed due to heavy compression or involvement with a large tumor. Observation in the responsible tract was performed at a region without enhancement on Gd-T1WI.

Imaging by 3DAC

All 3DAC scans were performed within 7 days before surgery. DWI scans were performed using a 3.0-T MRI system (Signa VH/I; GE Medical Systems, Milwaukee, WI, USA) using a standard head coil. A spin echo-type echo planar imaging sequence with diffusion gradients applied in three directions was used for DWI (repetition time (TR), 8000 ms; echo time (TE), 93 ms; matrix 128 × 128; field of view (FOV), 240 × 240 mm; 5 mm thickness; b factors, 1000 s/mm^2). The 3DAC image analysis after processing was performed in accordance with the methods described by Inoue et al. [19,20]. Images obtained using left-right, anterior-posterior and superior-inferior diffusion gradients were first transformed into grayscale levels, then color-coded using red, green, and blue, respectively. Colored images were then composited into a single colored image. Identical intensities of three colors, indicating isotropic diffusion, combined on images to appear as cancellation (white-out). In contrast, non-identical intensities of the three

Table 1. Patient characteristics

Case	Age/Sex	Tumor site	Hemiparesis Pre-op	Procedure	Hemiparesis Post-op
1	77 F	Lateral ventricle	3	biopsy	3
2	70 M	Corpus callosum	5	biopsy	5
3	70 M	Corpus callosum	4	biopsy	2
4	69 F	Parietal lobe	2	total	5
5	67 F	Parietal lobe	5	total	5
6	67 F	Parietal lobe	5	total	5
7	66 F	Frontal lobe	5	total	4
8	65 M	Parietal lobe	3	total	3
9	64 F	Basal ganglia	3	biopsy	2
10	64 M	Parietal lobe	5	total	5
11	63 M	Temporal lobe	5	total	5
12	63 F	Frontal lobe	5	total	6
13	56 F	Frontal lobe	4	biopsy	4
14	54 F	Frontal lobe	5	total	4
15	47 M	Temporal lobe	5	total	6
16	44 F	Corpus callosum	3	biopsy	2
17	41 F	Thalamus	5	subtotal	6
18	31 F	Frontal lobe	1	subtotal	5

Total, total removal; Subtotal, subtotal removal; Pre-op, preoperative; Post- op, postoperative.

colors, which are indicative of anisotropic diffusion, appear as the color showing the greatest strength and direction of the diffusion gradient. Thus, nerve fibers running left-right (x-axis), anterior-posterior (y-axis) and superior-inferior (z-axis) appear as green, blue and red, respectively. Mixed colors indicate oblique orientation of nerve fibers.

On 3DAC images, the same region of the pyramidal tract as the responsible tract defined on PDWI was observed in all patients, and patients were classified into three groups: (1) 'fine' group, in which the tract was observed without any change in color, compared with the pyramidal tract on the contralateral side of the same slice; (2) 'dark' group, in which color of the tract was obscure and dark; and (3) 'absent' group, in which tract could not be observed due to strong compression or involvement with a large tumor bulk.

FA value

DTI was performed using a 3.0-T MRI system (Signa VH/I; GE Medical Systems) with a standard head coil. A spin echo type echo planar imaging sequence with diffusion gradients applied in six directions was used for DTI (TR, 10,000 ms; TE, 84 ms; matrix, 256 × 260; FOV, 240 mm^2; 6 mm thickness, 2 mm gap; b factors, 800 s/mm^2). All patients also underwent conventional spin echo T1- and T2-WI prior to DTI, and T1WI with contrast medium after DTI. All image analyses after processing were performed on a scanner console using a subprogram of the Functool™ image analysis software (General Electric Medical Systems, Buc, France).

The FA values were measured at pyramidal tracts of the pathological and non-pathological sides. Regions of interest (ROI) were placed at the same region of the pyramidal tract as the responsible tract estimated on PDWI and 3DAC, and at the symmetrical region on the pyramidal tract of the non-pathological side. ROIs were automatically transferred onto co-registered FA maps constructed from DTI. FA values were then calculated for each patient using the modified Functool image analysis software. FA value was identified as the mean of values derived for every pixel in a given ROI. Statistical significance was established at the $P < 0.05$ level in all analyses.

Results

Findings of PDWI and 3DAC (Table 2)

The tract responsible for hemiparesis was the corona radiata in 14 patients, and the internal capsule in four patients. On PDWI, the finding of 'clear' in the responsible tract was observed in five patients. Responsible tracts in 11 patients revealed findings of 'hyperintense'. On 3DAC, the responsible tract was 'fine' in 10 patients and 'dark' in six. The tract in two patients displayed findings of 'absent' for both PDWI and 3DAC. All patients for whom PDWI showed findings of 'clear' demonstrated finding of 'fine' on 3DAC. When PDWI showed 'hyperintense', 3DAC demonstrated either 'fine' or 'dark'. As a result, patients could be classified into four groups (Table 2): Group A, 'clear' on PDWI and 'fine' on 3DAC ($n = 5$, 28%); Group B, 'hyperintense' on PDWI and 'fine' on 3DAC ($n = 5$, 28%); Group C, 'hyperintense' on PDWI and 'dark' on 3DAC ($n = 6$, 33%); and Group D, 'absent' on both procedures ($n = 2$, 11%).

Illustrative cases

Case 17 – Group A: The internal capsule was the tract responsible for hemiparesis, revealing 'clear' findings without hyperintense foci on PDWI, and 'fine' without any change in color compared to the contralateral side on 3DAC (Figure 1a–c).

Table 2: Findings of PDWI, 3DAC and FA

Case	Responsible tract	PDWI	3 DAC	Group	FA value	
					Non-pathological tract	Responsible tract
1	Corona radiata	Hyperintense	Fine	B	0.76	0.61
2	Corona radiata	Hyperintense	Dark	C	0.82	0.65
3	Corona radiata	Hyperintense	Dark	C	0.50	0.17
4	Corona radiata	Hyperintense	Fine	B	0.58	0.38
5	Corona radiata	Clear	Fine	A	0.57	0.54
6	Corona radiata	Hyperintense	Fine	B	0.52	0.45
7	Corona radiata	Hyperintense	Dark	C	0.69	0.23
8	Corona radiata	Hyperintense	Dark	C	0.65	0.36
9	Internal capsule	Hyperintense	Dark	C	0.56	0.39
10	Corona radiata	Hyperintense	Fine	B	0.62	0.66
11	Internal capsule	Clear	Fine	A	0.68	0.64
12	Corona radiata	Absent	Absent	D	0.77	0.53
13	Corona radiata	Clear	Fine	A	0.77	0.73
14	Corona radiata	Hyperintense	Dark	C	0.62	0.26
15	Internal capsule	Clear	Fine	A	0.65	0.67
16	Corona radiata	Hyperintense	Fine	B	0.67	0.65
17	Internal capsule	Clear	Fine	A	0.62	0.55
18	Corona radiata	Absent	Absent	D	0.49	0.46

Case 10 – Group B: In this case, the corona radiata was the responsible tract, displaying findings of 'hyperintense' on PDWI, and 'fine' on 3DAC (Figures 2a–c).

Case 7 – Group C: The corona radiata was the responsible tract, displaying findings of 'hyperintense' on PDWI, and 'dark' on 3DAC (Figure 3a–c). The patient underwent gross total removal of tumor bulk. Gd-T1WI at 3 months after surgery revealed a recurrent lesion in the same region as the slight dark lesion on initial 3DAC (Figure 4a), and 3DAC identified a black lesion in the area corresponding to the Gd-enhanced lesion (Figure 4b).

Case 18 – Group D: The corona radiata was the responsible tract, but could not be observed on either PDWI or 3DAC (Figure 5a–c).

FA value

Mean FA value of the pyramidal tract on the non-pathological side was 0.64 ± 0.10 (range, 0.49–0.77). In the responsible tracts, FA value ranged widely from 0.17 to 0.73 (Table 2). Comparison between FA values of non-pathological tract and responsible tract for each group was performed using paired *t*-tests. No significant

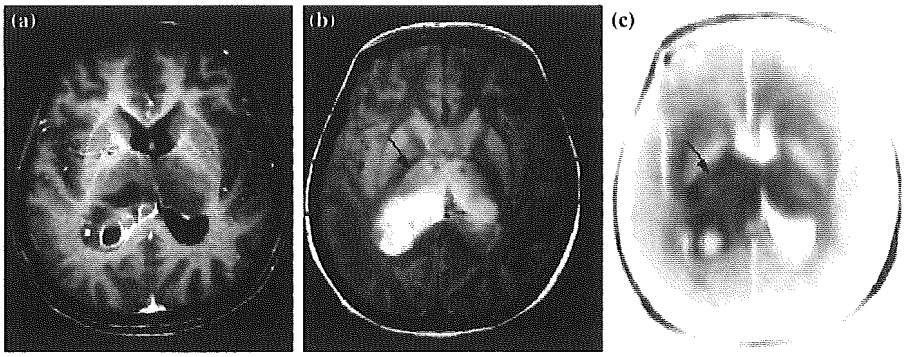

Figure 1. Conventional MRI and 3DAC in Case 17. (a) Gd-T1WI demonstrates glioblastoma situated in the right thalamus. (b) PDWI clearly shows the internal capsule as the tract responsible for hemiparesis, ipsilateral to the tumor (arrow). (c) Internal capsule is shown on 3DAC by absence of color change compared to contralateral side (arrow).

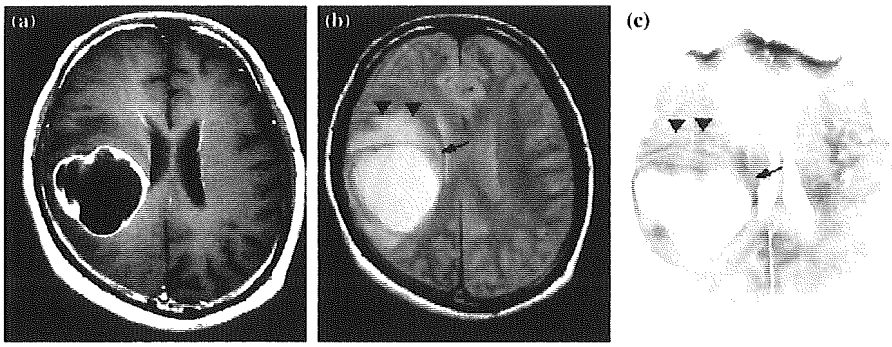

Figure 2. Conventional MRI and 3DAC in Case 10. (a) Gd-T1WI demonstrates a cystic-shaped glioblastoma situated in the right parietal lobe. (b) PDWI shows a hyperintense focus in the corona radiata as the responsible tract (arrow), and subcortical white matter surrounding the tumor, suggesting a perifocal edema (arrowhead). (c) 3DAC demonstrates no change in color for both corona radiata (arrow) and subcortical white matter surrounding the tumor, corresponding to a hyperintense focus on PDWI (arrowhead). Fluid within the cystic lesion is shown as an area of whiteout, as is cerebrospinal fluid within the lateral ventricle.

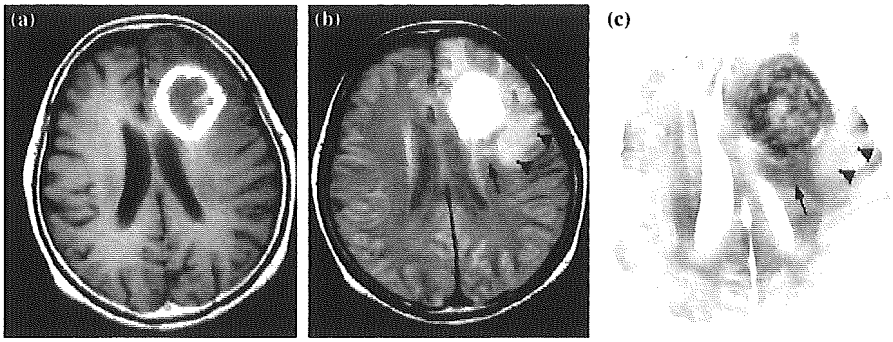

Figure 3. Conventional MRI and 3DAC in Case 7. (a) Gd-T1WI shows glioblastoma situated in the left frontal lobe. (b) PDWI demonstrates hyperintense foci, with corona radiata behind the tumor bulk (arrow), as the responsible tract, and subcortical white matter surrounding the tumor bulk (arrowhead). (c) 3DAC demonstrates slight darkness on the corona radiata (arrow), whereas white matter surrounding the tumor bulk displays faint coloration (arrowhead). The tumor bulk is darker than the responsible tract.

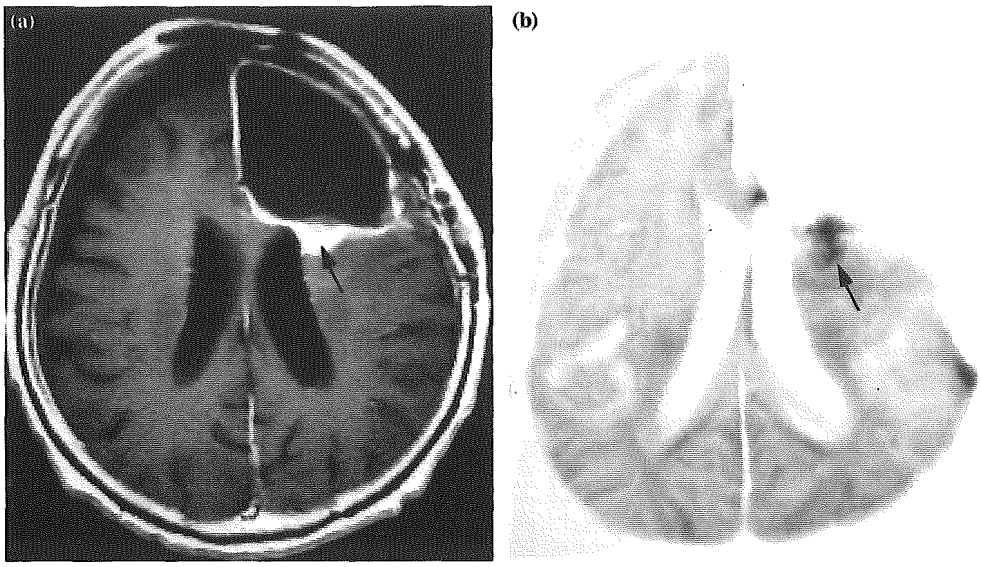

Figure 4. Conventional MRI and 3DAC of Case 7 at recurrence. (a) Gd-T1WI shows markedly enhanced mass suggesting recurrent glioblastoma in the anterior corona radiata, corresponding to the slightly darkened area in Figure 3C (arrow). (b) Recurrent glioblastoma shown as enhancement on Gd-T1WI appears black on 3DAC (arrow).

differences were found in Group A, B or D, whereas FA value was significantly lower for the responsible tract than for the non-pathological tract in Group C (Table 3).

Estimations of hemiparesis

Degree of preoperative hemiparesis varied from stage 4 to 5 in Group A, stage 2 to 5 in Group B, stage 3 to 5 in Group C and stage 1 to 5 in Group D (Table 1). Although hemiparesis before surgery tended to be more likely to be mild in Group A than in the other groups, no significant differences were identified between groups when hemiparesis was compared using the Kruskal–Wallis test ($P = 0.5$). In addition, no significant differences in postoperative hemiparesis among the four groups were identified using the Kruskal–Wallis test ($P = 0.07$). When limited to 12 patients who underwent either total or subtotal removal, improvement of hemiparesis after surgery was seen in two of the four patients in Group A, one of the three patients in Group B and all two patients in Group D. Hemiparesis did not deteriorate in any patient after surgery in these three groups. In contrast, no patients in Group C experienced improved hemiparesis after surgical intervention, and deterioration was observed in two of the three patients. Nevertheless, no significant differences in frequency of improvement were identified among the four groups using the χ^2 test for independence ($P = 0.16$). In the same 12 patients mentioned above, degree of hemiparesis before and after surgery was compared between seven patients in Group A or B and three patients in Group C, using the Mann–Whitney *U*-test. No significant difference in degree of hemiparesis before surgery was identified between Group A /B and Group C

Table 3. Comparison of FA values between non-pathological and responsible tracts for each group

Group	FA value (mean ± SD)		
	Non-pathological tract	Responsible tract	*P*
A	0.66 ± 0.08	0.63 ± 0.08	0.09
B	0.63 ± 0.09	0.55 ± 0.13	0.14
C	0.64 ± 0.11	0.34 ± 0.17	0.01
D	0.63 ± 0.20	0.50 ± 0.05	0.42

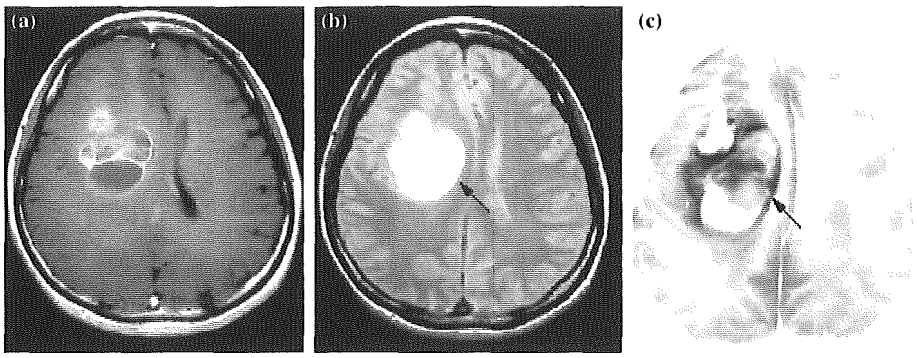

Figure 5. MR images and 3DAC in Case 18. (A) Gd-T1WI shows a huge glioblastoma in the right frontal lobe. Neither PDWI (B) nor 3DAC (C) revealthe corona radiata, due to the presence of a huge tumor. Whether the corona radiata was not apparent due to heavy compression or invasion of tumor bulk was unclear.

($P = 0.7$), while degree of hemiparesis after surgery in Group A/B was significantly milder than in Group C ($P = 0.02$).

Discussion

In the present study, 3DAC allowed clear depiction of the pyramidal tracts of the non-pathological side in all patients. These findings confirm previous reports that 3DAC offers a reliable technique for visualizing the pyramidal tracts [18,20]. The 3DAC demonstrated various findings in responsible pyramidal tracts. When PDWI clearly showed the responsible tracts without hyperintense foci, 3DAC findings also demonstrated fine detail of the responsible tracts without any change in color, as with Case 17 in Group A (Figure 1a–c). Furthermore, all patients in Group A presented with mild preoperative hemiparesis of stage 4 or 5, although no significant difference between degree of preoperative hemiparesis in Group A and the other groups was noted. When symptoms appear due to expansion of glioma, the more malignant peripheral areas of the tumor invade into dense fibers, such as the pyramidal tract. The tumor initially grows faster in one direction, as a result of fiber density, and disrupts the fibers in the next stage [29]. Results of PDWI, 3DAC and degree of hemiparesis suggest that pyramidal tracts in Group A patients did not appear to be disrupted by tumor, even if invasion to the pyramidal tract had occurred. The finding that mean FA value of the responsible tract for Group A did not differ significantly from that of the contralateral side might support this possibility that the tract is not disrupted (Table 3). Thus, 3DAC might not offer any advantages for evaluating condition of the pyramidal tract in patients for whom the responsible tract can be clearly visualized on PDWI.

When PDWI showed hyperintense foci in the responsible pyramidal tract, 3DAC demonstrated the responsible tract either as showing no change of color compared with the contralateral side, such as Case 10 in Group B (Figure 2c), or as showing darkness, like Case 7 in Group C (Figure 3c). Findings of obscured, dark areas in the pyramidal tract on 3DAC have been observed in patients with cerebral infarction. Cytotoxic edema, axonal swelling and Wallerian degeneration, all of which are seen in ischemic lesions and diffuse axonal injuries [30–32], have been suggested as hindering water diffusion, thereby creating darkened areas in the pyramidal tract on 3DAC [20,33]. In contrast, most edema surrounding a tumor, which predominantly comprises extracellular edema, should isotropically accelerate water diffusion, as extracellular edema leads to increased amounts of interstitial water [34,35]. The present study suggests that widespread hyperintense foci surrounding a tumor on PDWI result from extracellular edema rather than tumor invasion, as either no or only faint color change was apparent on 3DAC (Figures 2c and 3c, arrowheads). High cellular and/or nuclear densities have been recognized a factor hindering water diffusion [36–38]. In fact, tumor bulks displaying high cellular density are shown as areas of darkness on 3DAC in the present study. Conversely, we believe that darkened regions in the responsible tract of patients with glioblastoma resulted from a large obstruction to water diffusion due to invasion by tumor cells. Mean FA of the responsible tract for Group C was significantly decreased from that of the non-pathological side (Table 3). This finding does not directly indicate high cellular density, but suggests that the responsible tract has been largely destroyed by tumor invasion. As shown in Case 7, a dark lesion progressed on 3DAC, corresponding to a finely enhanced recurrent mass on Gd-T1WI (Figure 4a, b). This observation might also support our hypothesis that a darkened area on 3DAC is induced by tumor invasion. Furthermore, this finding suggests that 3DAC can predict infiltration of tumor cells into the pyramidal tract earlier than Gd-T1WI can. However, the responsible tract in Group B patients displayed coloration without darkness on 3DAC. No significant difference in mean FA existed between the responsible and non-pathological tracts, although mean FA of the responsible tract tended to be slightly lower than that of the non-pathological tract (Table 3). These findings suggest that the responsible tract in Group B patients was not heavily invaded or destroyed by tumor, unlike Group C. The finding of improved hemiparesis after mass reduction in one patient in Group B, compared to no patients in Group C, might support our speculation. If a hyperintense focus surrounding glioblastoma spreads to the pyramidal tract in conventional MRI on patients with hemiparesis, clinicians would hesitate over whether the pyramidal tract has been disrupted by tumor invasion. Degree of hemiparesis might not offer a predictor of pyramidal tract condition, because degree of hemiparesis before surgery did not differ significantly among the four groups. We believe that 3DAC may prove useful for examining hyperintense foci surrounding glioblastoma that have spread to the pyramidal tract on PDWI.

In Group D, we were unable to speculate on the condition of the responsible tract, as the tract was absent on 3DAC. FA value and improvement of hemiparesis after a mass reduction may lead to the speculation that the responsible tracts in Group D patients have not been largely destroyed by tumor invasion. However, 3DAC does not offer a predictor of pyramidal tract condition when the tract is not observed such as in Group D.

The present study is limited with regard to interpretations of 3DAC images. We did not undertake histological observations of responsible pyramidal tracts, and thus the amount of tumor cell invasion required for the responsible tract to become abnormally dark as in Group C remains unclear. If we assume that the responsible tracts of both Groups A and B were invaded by tumor cells, a greater degree of invasion may be present in Group B than in Group A, as PDWI revealed hyperintense foci in Group B. Again, the real differences causing these varying results remain unclear. Histological investigations into correlations between degrees of

cellular density, fiver destruction, hyperintensity on PDWI and color on 3DAC are warranted.

Conclusion

No previous reports have revealed that 3DAC findings allow suggestions as to the status of the pyramidal tract adjacent to glioblastoma. Our findings suggest that 3DAC imaging is useful for evaluating condition of the pyramidal tract, in terms of potential extensive destruction by tumor invasion, when hyperintense foci surrounding the tumor spread to the pyramidal tract on conventional MRI for glioblastoma patients with hemiparesis. Use of 3DAC with DWI will likely offer a feasible option for preoperative examination in glioblastoma patients.

Acknowledgements

This study was supported in part by the Advanced Medical Science Center, Iwate Medical University.

References

1. Gallen CC, Sobel DF, Waltz T, Aung M, Copeland B, Schwartz BJ, Hirschkoff EC, Bloom FE. Noninvasive presurgical neuromagnetic mapping of somatosensory cortex. Neurosurgery 33: 260–268, 1993
2. Atlas SW, Howard RS 2nd, Maldjian J, Alsop D, Detre JA, Listerud J, D'Esposito M, Judy KD, Zager E, Stecker M: Functional magnetic resonance imaging of regional brain activity in patients with intracerebral gliomas: findings and implications for clinical management. Neurosurgery 38: 329–338, 1996
3. Cosgrove GR, Buchbinder BR, Jiang H: Functional magnetic resonance imaging for intracranial navigation. Neurosurg Clin N Am 7: 313–322, 1996
4. Berger MS, Rostomily RC: Low grade gliomas functional mapping resection strategies, extent of resection, and outcome. J Neuro-Oncol 34: 85–101, 1997
5. Nakasato N, Kumabe T, Kanno A, Ohtomo S, Mizoi K, Yoshimoto T: Neuromagnetic evaluation of cortical auditory function in patients with temporal lobe tumors. J Neurosurg 86: 610–618, 1997
6. Karibe H, Shimizu H, Tominaga T, Koshu K, Yoshimoto T: Diffusion-weighted magnetic resonance imaging in the early evaluation of corticospinal tract injury to predict functional motor outcome in patients with deep intracerebral hemorrhage. J Neurosurg 92: 58–63, 2000
7. Krings T, Reinges MH, Thiex R, Gilsbach JM, Thron A: Functional and diffusion-weighted magnetic resonance images of space-occupying lesions affecting the motor system: imaging the motor cortex and pyramidal tracts. J Neurosurg 95: 816–824, 2001
8. Cooper RL, Chang DB, Young AC, Martin CJ, Ancker-Johnson D: Restricted diffusion in biophysical systems. Experiment Biophys J 14: 161–177, 1974
9. Le Bihan D: Diffusion, perfusion and functional magnetic resonance imaging. J Mal Vasc 20: 203–214, 1995
10. Schaefer PW, Grant PE, Gonzalez RG: Diffusion-weighted MR imaging of the brain. Radiology 217: 331–345, 2000
11. Aoyama H, Kamada K, Shirato H, Takeuchi F, Kuriki S, Iwasaki Y, Miyasaka K: Visualization of the corticospinal tract pathway using magnetic resonance axonography and magnetoencephalography for stereotactic irradiation planning of arteriovenous malformations. Radiother Oncol 68: 27–32, 2003
12. Holodny AI, Schwartz TH, Ollenschleger M, Liu WC, Schulder M: Tumor involvement of the corticospinal tract: diffusion magnetic resonance tractography with intraoperative correlation. J Neurosurg 95: 1082, 2001
13. Parmar H, Sitoh YY, Yeo TT: Combined magnetic resonance tractography and functional magnetic resonance imaging in evaluation of brain tumors involving the motor system. J Comput Assist Tomogr 28: 551–556, 2004
14. Watanabe T, Honda Y, Fujii Y, Koyama M, Matsuzawa H, Tanaka R: Three-dimensional anisotropy contrast magnetic resonance axonography to predict the prognosis for motor function in patients suffering from stroke. J Neurosurg 94: 955–960, 2001
15. Watanabe T, Honda Y, Fujii Y, Koyama M, Tanaka R: Serial evaluation of axonal function in patients with brain death by using anisotropic diffusion-weighted magnetic resonance imaging. J Neurosurg 56–60, 2004
16. Witwer BP, Moftakhar R, Hasan KM, Deshmukh P, Haughton V, Field A, Arfanakis K, Noyes J, Moritz CH, Meyerand ME, Rowley HA, Alexander AL, Badie B: Diffusion-tensor imaging of white matter tracts in patients with cerebral neoplasm. J Neurosurg 97: 568–575, 2002
17. Nakada T, Matsuzawa H, Kwee IL: Magnetic resonance axonography of the rat spinal cord. Neuroreport 27: 2053–2056, 1994
18. Nakada T, Nakayama N, Fujii Y, Kwee IL: Clinical application of three-dimensional anisotropy contrast magnetic resonance axonography. Technical note. J Neurosurg 90: 791–795, 1999
19. Inoue T, Shimizu H, Yoshimoto T: Imaging the pyramidal tract in patients with brain tumors. Clin Neurol Neurosurg 101: 4–10, 1999
20. Inoue T, Shimizu H, Yoshimoto T, Kabasawa H: Spatial functional distribution in the corticospinal tract at the corona radiata: a three-dimensional anisotropy contrast study. Neurol Med Chir 41: 293–299, 2001
21. Coenen VA, Krings T, Mayfrank L, Polin RS, Reinges MH, Thron A, Gilsbach JM: Three-dimensional visualization of the pyramidal tract in a neuronavigation system during brain tumor surgery: first experiences and technical note. Neurosurgery 49: 86–93, 2001
22. Holodny AI, Schwartz TH, Ollenschleger M, Liu WC, Schulder M: Tumor involvement of the corticospinal tract: diffusion magnetic resonance tractography with intraoperative correlation. J Neurosurg 95: 1082, 2001
23. Kamada K, Houkin K, Iwasaki Y, Takeuchi F, Kuriki S, Mitsumori K, Sawamura Y: Rapid identification of the primary motor area by using magnetic resonance axonography. J Neurosurg 97: 558–567, 2002
24. Kashimura H, Inoue T, Ogasawara K, Ogawa: Preoperative evaluation of neural tracts by use of three-dimensional anisotropy contrast imaging in a patient with brainstem cavernous angioma: technical case report. Neurosurgery 52: 1226–1230, 2003
25. Darwin RH, Drayer BP, Riederer SJ, Wang HZ, MacFall JR: T2 estimates in healthy and diseased brain tissue: a comparison using various MR pulse sequences. Radiology 160: 375–381, 1986
26. Papadakis NG, Xing D, Houston GC, Smith JM, Smith MI, James MF, Parsons AA, Huang CL, Hall LD, Carpenter TA: A study of rotationally invariant and symmetric indices of diffusion anisotropy. Magn Reson Imaging 17(6): 881–892, 1999
27. Sorensen AG, Wu O, Copen WA, Davis TL, Gonzalez RG, Koroshetz WJ, Reese TG, Rosen BR, Wedeen VJ, Weisskoff RM: Human acute cerebral ischemia: detection of changes in water diffusion anisotropy by using MR imaging. Radiology 212(3): 785–792, 1999
28. Brunnstrom S: Motor testing procedures in hemiplegia. J APTA 46: 357–375, 1966
29. Yasargil MG: Microneurosurgery IV A (In 4 volumes). Georg Thieme, Stuttgart/New York Verlag (for distribution in Japan: Nankodo Company, Tokyo), 1993, pp. 127–134
30. Barzo P, Marmarou A, Fatouros P, Hayasaki K, Corwin F: Contribution of vasogenic and cellular edema to traumatic brain

swelling measured by diffusion-weighted imaging. J Neurosurg 87: 900–907, 1997
31. Castillo M, Mukherji SK. Early abnormalities related to postinfarction Wallerian degeneration: evaluation with MR diffusion-weighted imaging. J Comput Assist Tomogr 23: 1004–1007, 1999
32. Mukherjee P, Bahn MM, McKinstry RC, Shimony JS, Cull TS, Akbudak E, Snyder AZ, Conturo TE: Differences between gray matter and white matter water diffusion in stroke: diffusion-tensor MR imaging in 12 patients. Radiology 215: 211–220, 2000
33. Igarashi H, Katayama Y, Tsuganezawa T, Yamamuro M, Terashi A, Owan C: Three-dimensional anisotropy contrast (3DAC) magnetic resonance imaging of the human brain: application to assess Wallerian degeneration. Intern Med 37: 662–668, 1998
34. Gonatas NK, Zimmerman HM, Levine S: Ultrastructure of inflammation with edema in the rat brain. Am J Pathol 42: 455–469, 1963
35. Schwartz RB, Mulkern RV, Gudbjartsson H, Jolesz F. Diffusion-weighted MR imaging in hypertensive encephalopathy: clues to pathogenesis. AJNR Am J Neuroradiol 19: 859–862, 1998
36. Sugahara T, Korogi Y, Kochi M, Ikushima I, Shigematu Y, Hirai T, Okuda T, Liang L, Ge Y, Komohara Y, Ushio Y, Takahashi M: Usefulness of diffusion-weighted MRI with echo-planar technique in the evaluation of cellularity in gliomas. J Magn Reson Imaging 9: 53–60, 1999
37. Okamoto K, Ito J, Ishikawa K, Sakai K, Tokiguchi S: Diffusion-weighted echo-planar MR imaging in differential diagnosis of brain tumors and tumor-like conditions. Eur Radiol 10: 1342–1350, 2000
38. Gauvain KM, McKinstry RC, Mukherjee P, Perry A, Neil JJ, Kaufman BA, Hayashi RJ. Evaluating pediatric brain tumor cellularity with diffusion-tensor imaging. AJR Am J Roentgenol 177: 449–454, 2002

Address for offprints: Takaaki Beppu, Department of Neurosurgery, Iwate Medical University, 19—1, Uchimaru, Morioka 020—8505, Japan; Tel.: 019-651-5111; Fax: 019-625-8799; E-mail: tbeppu@iwate-med.ac.jp

ELSEVIER

Clinical Neurology and Neurosurgery 107 (2005) 174–180

Clinical Neurology and Neurosurgery

www.elsevier.com/locate/clineuro

Diffusion tensor imaging for preoperative evaluation of tumor grade in gliomas

Takashi Inoue[a,*], Kuniaki Ogasawara[a], Takaaki Beppu[a], Akira Ogawa[a], Hiroyuki Kabasawa[b]

[a] *Department of Neurosurgery, Iwate Medical University School of Medicine, 19-1 Uchimaru, Morioka, Iwate 020-8505, Japan*
[b] *GE Yokogawa Medical Systems, Tokyo, Japan*

Received 15 September 2003; received in revised form 24 May 2004; accepted 8 June 2004

Abstract

The relationship between water diffusion parameters measured using diffusion tensor imaging (DTI) and histological malignancy of gliomas was investigated.

DTI was performed using a 3.0 T MR scanner in 41 consecutive patients with histologically proven gliomas. Fractional anisotropy (FA) and mean diffusivity (MD) were calculated and compared with the WHO classification of the gliomas.

The FA values of grade 1 gliomas (0.150 ± 0.017) were significantly lower than those of grade 3 (0.23 ± 0.033) or grade 4 gliomas (0.229 ± 0.033) ($P < 0.0001$, respectively). The FA values of grade 2 gliomas (0.159 ± 0.018) were significantly lower than those of grade 3 or grade 4 gliomas ($P = 0.0002$, $P < 0.0001$, respectively). The FA threshold between low grade and high grade gliomas was 0.188. The MD values of grade 1 gliomas ($1619.1 \pm 157.4 \times 10^{-6}$ mm^2/s) were significantly higher than those of grade 3 ($1084.5 \pm 218.9 \times 10^{-6}$ mm^2/s) ($P = 0.0036$) or grade 4 gliomas ($1098.0 \pm 291.6 \times 10^{-6}$ mm^2/s) ($P = 0.0002$). The MD values were not correlated with the other grades of glioma.

FA values can distinguish between high grade and low grade gliomas. This is useful in deciding the surgical strategy or selecting the site of stereotactic biopsy.

Keywords: Diffusion tensor imaging; Glioma; Malignancy

1. Introduction

Gliomas are the most common primary neoplasms of the central nervous system [1]. The prognosis for patients with high grade gliomas has remained poor despite improvements in radiation and chemotherapy [2,3]. Accurate preoperative diagnosis of the tumor grade is important for the determination of appropriate treatment strategies [4]. Magnetic resonance (MR) spectroscopy [5–8], single photon emission computed tomography [9–13], or positron emission tomography [9–11] have all been used for the preoperative evaluation of glioma malignancy. However, MR spectroscopy has limitations in spatial resolution and heterogeneous lesions are difficult to assess [7], whereas imaging methods using radioactive isotopes are invasive and involve handling problems.

Diffusion tensor imaging (DTI) can measure the directionality (anisotropy) and the magnitude (diffusivity) of water diffusion in vivo [14]. Fractional anisotropy (FA) and mean diffusivity (MD) are the quantitative indices for anisotropy and diffusivity, respectively [15]. The microstructural organization of the brain tissue affects the molecular motion of water. Therefore, the FA and MD reflect microstructural changes of tissue caused by damage from degenerative disease, brain ischemia and brain tumors [16–21]. The histological diagnosis of glioma malignancy is based on the presence of nuclear heteromorphism, nuclear mitosis, endothelial proliferation, and necrosis [22]. These characteristics may affect the FA and MD values of gliomas.

* Corresponding author. Tel.: +81 19 651 5111; fax: +81 19 625 8799.
E-mail address: tainoue@iwate-med.ac.jp (T. Inoue).

0303-8467/$ – see front matter © 2004 Elsevier B.V. All rights reserved.
doi:10.1016/j.clineuro.2004.06.011

Table 1
Patient characteristics and tumor grades, using the WHO classification

Case no.	Age	Sex	Grade	FA value	MD value × 10^{-6} mm^2/s
1	7	F	G1	0.161	1552.6
2	10	F	G1	0.140	1395.9
3	15	F	G1	0.152	1706.3
4	23	F	G1	0.165	1525.9
5	6	M	G1	0.150	1779.7
6	27	M	G1	0.154	1448.7
7	43	M	G1	0.112	1797.73
8	69	M	G1	0.163	1745.91
9	35	F	G2	0.158	1087.9
10	46	F	G2	0.172	1010.1
11	48	F	G2	0.144	969.9
12	2	M	G2	0.176	1588.0
13	28	M	G2	0.154	1403.2
14	33	M	G2	0.163	1251.3
15	40	M	G2	0.122	1380.94
16	59	M	G2	0.181	1407.37
17	60	M	G2	0.157	1493.2
18	43	F	G3	0.231	1328.5
19	68	F	G3	0.237	778.8
20	4	M	G3	0.227	951.9
21	39	M	G3	0.206	1270.26
22	51	M	G3	0.203	957.3
23	60	M	G3	0.293	1220.12
24	41	F	G4	0.214	877.7
25	44	F	G4	0.195	1085.8
26	54	F	G4	0.199	972.11
27	58	F	G4	0.250	874.3
28	68	F	G4	0.218	612.7
29	68	F	G4	0.207	1146.8
30	68	F	G4	0.319	1385.69
31	69	F	G4	0.196	1278.4
32	77	F	G4	0.220	1224.8
33	15	M	G4	0.219	694.7
34	47	M	G4	0.225	865.2
35	56	M	G4	0.216	1328.77
36	61	M	G4	0.212	1326.9
37	63	M	G4	0.283	875.67
38	63	M	G4	0.232	1049.6
39	64	M	G4	0.204	1838.47
40	72	M	G4	0.257	1286.71
41	74	M	G4	0.251	1038.82

This study evaluates the relationship between the findings of DTI and the histological malignancy of gliomas.

2. Clinical material and methods

2.1. Patient population

This study included 41 consecutive patients (18 females and 23 males) aged 2–77 years (mean 46 years) treated at our institute between October 2000 and December 2002, who underwent DTI and had a histological diagnosis. No medical therapy was received for their tumor prior to imaging. The patient characteristics and tumor grades, using the WHO classification [23], are listed in Table 1. The study protocol was approved by the local ethical committee. All subjects gave written informed consent prior to the study.

2.2. MR imaging

All MR imaging used a Signa VH/i 3.0 T MR imaging system (General Electric Medical Systems, Milwaukee, WI) and standard head coil. A spin echo echo planar imaging (EPI) sequence with diffusion gradients applied in six directions ((*x*, *y*, z): (101), (−101), (011), (01 −1), (110) and (−110) direction, respectivery) was used for DTI: repetition time 10,000 ms, echo time 84 ms, matrix 256 × 260, field of view 240 mm, number of excitations 6, slice thickness 6 mm, gap 2 mm, and *b* factor 800 s/mm^2. All patients underwent conventional spin echo T1-weighted imaging with contrast medium after DTI.

2.3. Image analysis

All image post processing was performed on a scanner console using a subprogram, developed by one of the authors (H.K.), of the Functool^{TM} image analysis software (General Electric Medical Systems, Buc, France). The scalars invariants of the tensor, FA and MD, were derived for every pixel. The regions of interest (ROIs) were determined on the T2-weighted EPI scans, and were positioned on the solid portion of the lesions. In the enhanced tumors, the ROIs were confirmed to set the enhanced lesion on the T1 weighted images with contrast medium. The ROIs were automatically transferred onto the coregistered FA and MD maps (Fig. 1). Then, the FA and MD values were calculated for each patient.

2.4. Statistical analysis

The relationship between the FA or MD values and the tumor grade was evaluated with Scheffe's *F* test. Statistical significance was set at $P < 0.05$.

3. Results

DTI demonstrated the tumor mass and cystic lesions in all patients. Representative FA maps and T1-weighted images with contrast medium are shown in Fig. 2. The relationships between the FA or MD values and the tumor grade are shown in Figs. 3 and 4, respectively.

The FA values of grade 1 gliomas (0.150 ± 0.017) were significantly lower than those of grade 3 (0.23 ± 0.033) or grade 4 gliomas (0.229 ± 0.033) ($P < 0.0001$, respectively). The FA values of grade 2 gliomas (0.159 ± 0.018) were significantly lower than those of grade 3 or grade 4 gliomas ($P = 0.0002$, $P < 0.0001$, respectively). The FA threshold between low grade (grade 1 and 2) and high grade gliomas (grade 3 and 4) was 0.188 (Fig. 3). Differences between the

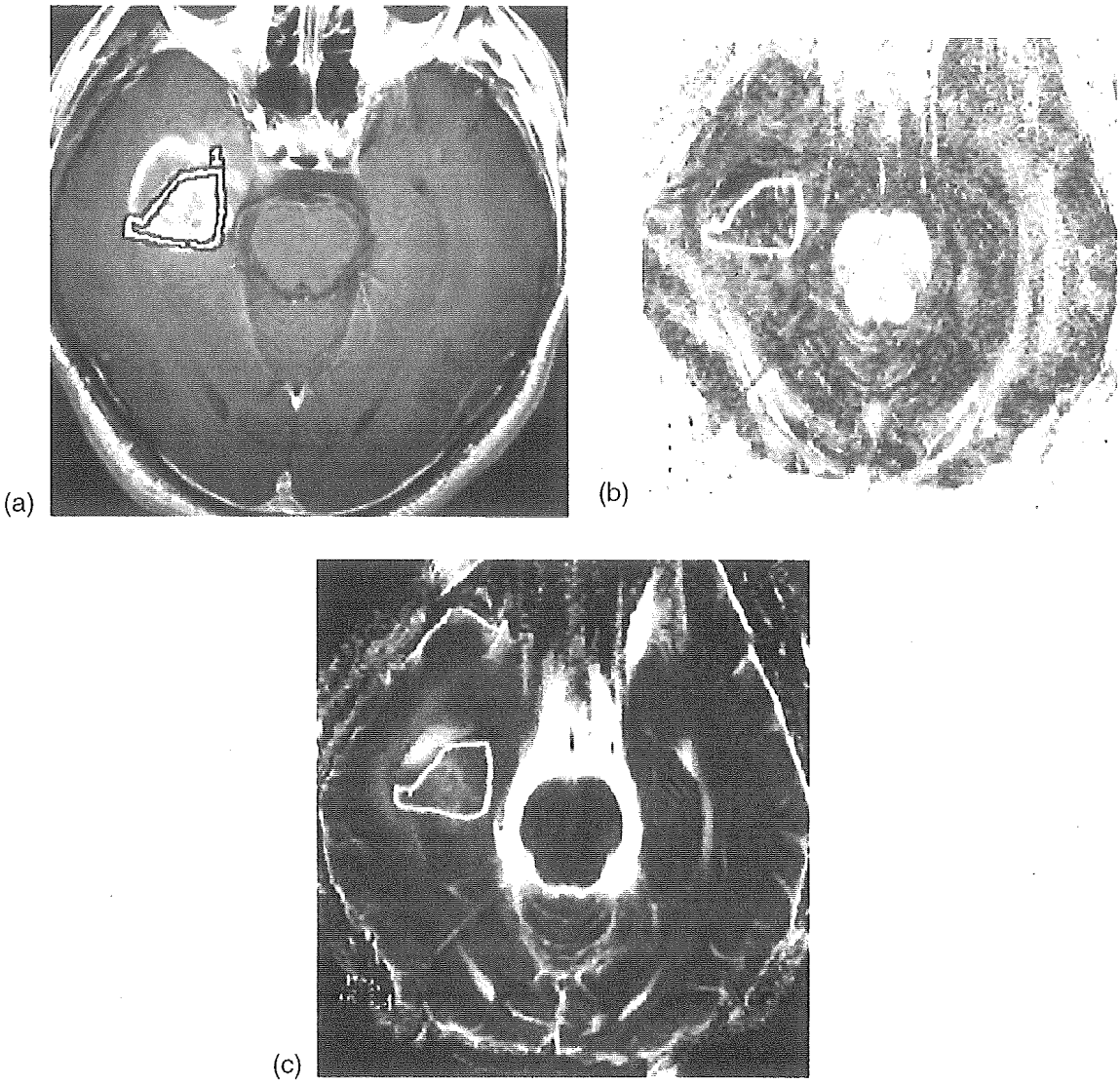

Fig. 1. (a) T1-weighted magnetic resonance (MR) image with contrast medium showing the region of interest (ROI) in the solid portion of the lesion. (b) Fractional anisotropy map showing the outline of the ROI traced automatically. (c) Mean diffusivity map showing the outline of the ROI traced automatically.

FA values of grades 1 and 2, or grades 3 and 4 were not significant.

The MD values of grade 1 gliomas ($1619.1 \pm 157.4 \times 10^{-6}$ mm^2/s) were significantly higher than those of grade 3 ($1084.5 \pm 218.9 \times 10^{-6}$ mm^2/s) ($P = 0.0036$) or grade 4 gliomas ($1098.0 \pm 291.6 \times 10^{-6}$ mm^2/s) ($P = 0.0002$). Differences between the MD values of grade 1 and 2 ($1288.0 \pm 220.2 \times 10^{-6}$ mm^2/s), 2 and 3, and 3 and 4 were not significant. There was no clear threshold value between low grade and high grade gliomas (Fig. 4).

4. Discussion

The primary finding of the present study was that the FA value could be used to distinguish high grade glioma from low grade glioma.

FA values have been investigated in patients with multiple sclerosis, amyotrophic lateral sclerosis, or leukoaraiosis, showing that the FA value is an indicator of the tissue damage of white matter [17–20,24]. The molecular movement of water is restricted by membranes in the brain [25]. The presence of myelinated fibers is an important factor in the underlying mechanisms of anisotropic diffusion [26]. Thus, damaged tissue in myelinated fibers may have reduced FA values. Anisotropy is always reduced in brain tumors [21]. In the present study, the FA values of gliomas were lower than those of subcortical white (0.76 ± 0.05) and gray (0.25 ± 0.1) matter [21], which corresponded with previous findings.

The present study showed that the FA values of high grade gliomas were significantly higher than those of low grade gliomas. High anisotropy implies that the tissue is symmetrically organized [21]. High grade glioma is histologically characterized by pseudo-palisading, endothelial

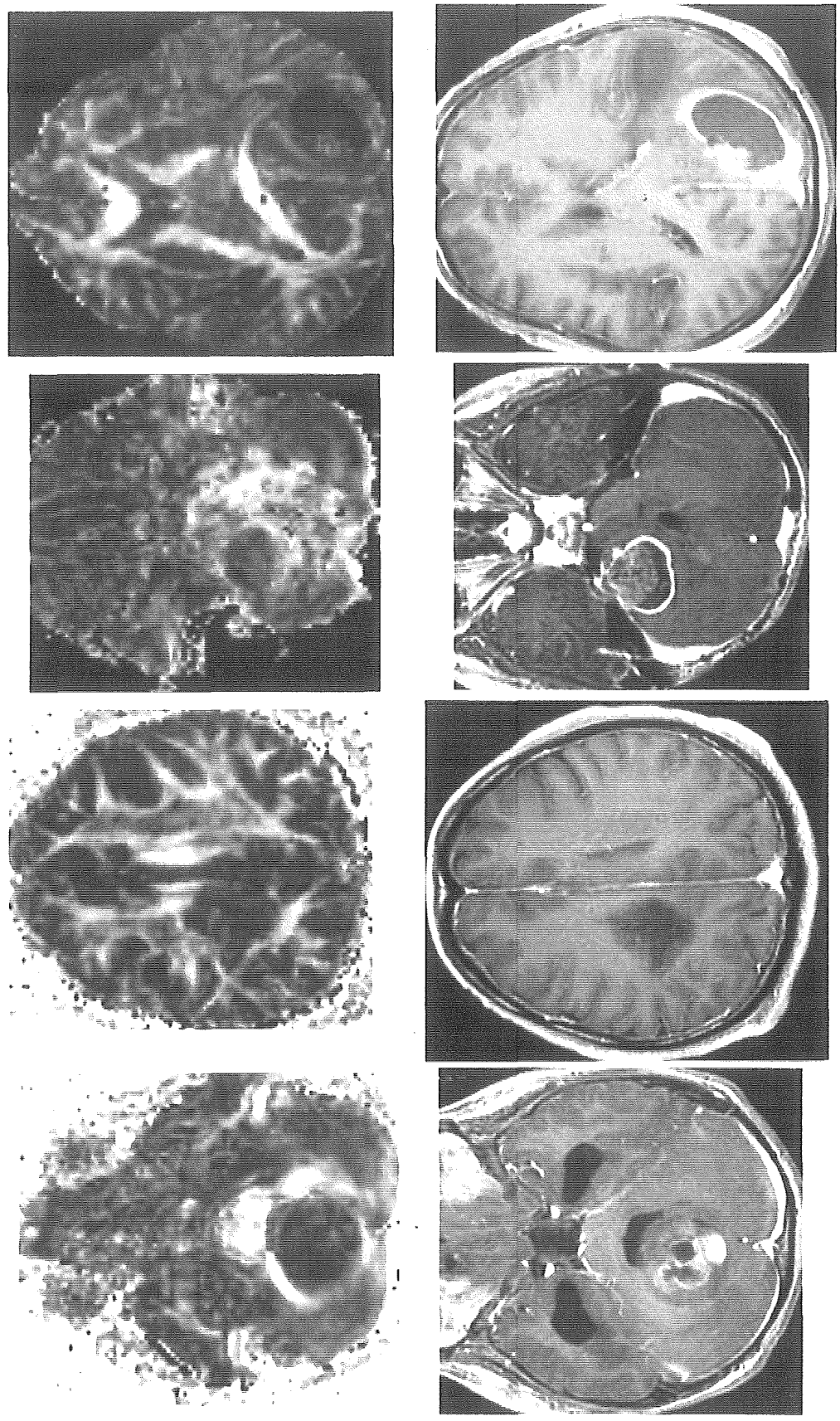

Fig. 2. Representative fractional anisotropy maps (upper row) and T1-weighted MR images with contrast medium (lower row).

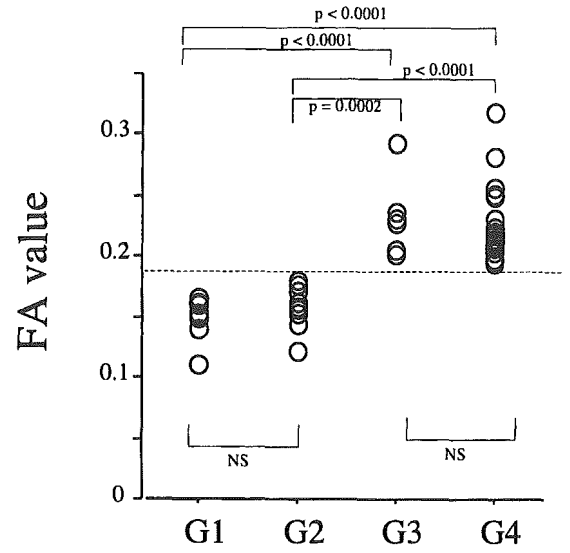

Fig. 3. Fractional anisotropy (FA) values and glioma grade. Dashed line, threshold between low grade (G1 and G2) and high grade gliomas (G3 and G4).

proliferation, or glomerular formation. The symmetric histological organization may influence the anisotropy and increase the FA value. However, high grade glioma is also characterized by necrosis. Actually, it was reported that the necrotic core of the high grade gliomas showed low FA values [27]. Therefore, in the present study we strictly limited the ROIs to be within the tumor body and to avoid the inclusion of large necrosis. Thus, our findings suggest that preoperative measurement of the FA values may predict the malignancy of gliomas, which may be useful in deciding the surgical strategy or selecting the site of stereotactic biopsy.

In the present study, the MD values of grade 1 gliomas were significantly higher than those of high grade gliomas.

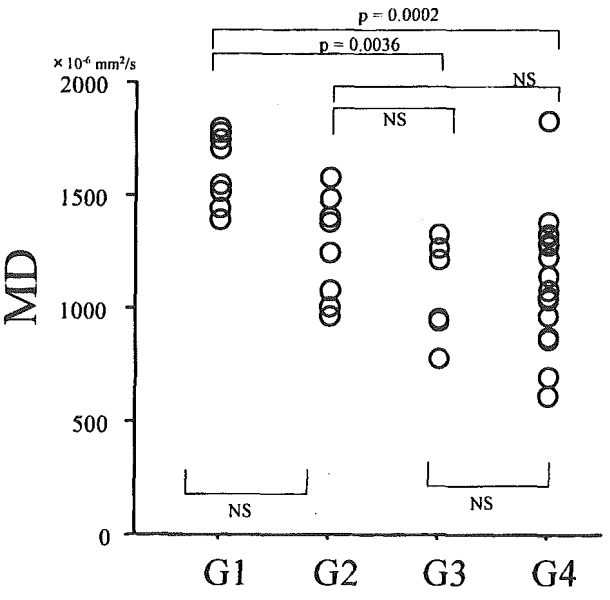

Fig. 4. Mean diffusivity (MD) values and glioma grade.

However, the other grades of glioma did not correlate with the MD values. Thus, the MD value was a poor predictor to distinguish the malignancy of gliomas in comparison with the FA value. MD values have been correlated with the histological cellularity of gliomas and are useful to distinguish low grade gliomas from high grade gliomas [4]. The exact reason for this discrepancy between previous findings and our results is difficult to assess, but there are several possible explanations. First, microstructural changes including cell swelling, shrinkage, or widening of the extracellular space can affect the MD values [28,29]. Second, low grade glioma may exhibit moderate or high cellularity [30,31]. Thus, the MD values may not correlate with the glioma grades.

Cystic changes or necrosis within lesions could decrease or increase FA and MD values, respectively. Therefore, we excluded that possibility by using high resolution DTI. High field MR imaging is useful to investigate fine anatomical structures [32,33], so cyst or necrosis within the tumor is easily differentiated from the solid portion.

Our study has some limitations regarding interpretation of the FA values. First is the normal variation in the FA values among different brain regions. For example, there is a more than 2-fold difference in the FA values between peripheral white matter such as neocortical association tracts and central commissural tracts such as the splenium of the corpus callosum [34,35]. If high grade gliomas tend to occur in deep white matter, they may have higher FA value. In fact, "butterfly gliomas" found at the splenium of the corpus callosum tend to be Grade IV glioma rather than Grade I or II gliomas. Second is the heterogeneity of the FA and the MD values within tumors. Although this may not cause serious problems in entirely homogenous tumors, discrepancy may have occurred between the ROIs and histologic samples in heterogeneous tumors. An image-guided technique, which was not applied in the present study for the purpose of tissue sampling, would improve spatial correlation between the samples examined by DTI and histologic examination. Third is that DTI did not cancel the perfusion effects. Tumor vascularity or microcirculation in the pathological tissue may affect the FA values. We should apply higher b value DTI to reduce the contribution of the perfusion effects [36–38]. However, higher b value DTI reduces the signal to noise ratio instead of reduction of the contribution of the perfusion effects. In our study, we used high resolution DTI to set the ROIs in the tumor bulk, not in the cystic or necrotic regions. Therefore, we used b value of 800 s/mm^2 in this investigation. Further investigation to compare the findings of DTI and histological examination is required.

5. Conclusion

Investigation of the relationship between DTI and histological malignancy of gliomas found that the FA value can